

## A NUMERICAL SIMULATION FOR PREDICTION OF INFRARED RADIATION EMITTED FROM PLAIN SURFACES WITH DIFFERENT GEOMETRIES

K.A. VAKILABADI\*

Department of Marine Faculty of Imam  
Khomeini Maritime University Iran  
Nowshahr, IRAN  
E-mail: Akbari.karim@gmail.com

H. MOAYERI and H. GHASSEMI

Department of Marine  
Faculty of Amirkabir University of Technology  
Tehran, IRAN  
E-mails: Sirhamid@aut.ac.ir; gasemi@aut.ac.ir

In this paper, infrared radiation exiting plain surfaces with different geometries is numerically simulated. Surfaces under consideration are assumed to have steady uniform heat generation inside. Moreover, the boundaries of the surfaces are considered to be at the surroundings temperature. Infrared radiation is calculated based on the temperature profile determined for the surface. The temperature profile of the surface is determined assuming the two dimensional heat conduction equations to govern the problem. The physical domain is transformed into the appropriate computational domain and the governing equation is mapped into the suitable forms in the new coordinate system of variables. After that the temperature profile of the surface is computed, the infrared radiation distribution of the surface is evaluated based on the equations given in the manuscript. The temperature profile as well as the IR images are given in the results section. It is concluded that the maximum value of infrared radiation of the surface occurs at the center. Moreover, it is concluded that among surfaces with equal areas, the one having the largest perimeter has the least value of IR at its center.

**Key words:** numerical simulation, infrared radiation, plain surfaces.

### 1. Introduction

Infrared radiation, IR, is the term used to identify the portion of radiant energy within red color and microwave in the electromagnetic spectrum. Every object either in vacuum or any material medium emits thermal energy in the form of electromagnetic waves. Included in the electromagnetic spectrum is a variety of wavelengths from a few nanometers to an order of kilometer. Gamma rays, X rays, visible light, microwaves and radio waves are all constituents of the electromagnetic spectrum. The electromagnetic waves lying within a tiny bandwidth of about  $0.4 \mu\text{m}$ , starting at  $0.3 \mu\text{m}$  for violet color, represent the visible light region. At the end of this bandwidth red color of  $0.7 \mu\text{m}$  in wavelength is seen. The infrared waves begin just after red color. Infrared waves, though starting from just about a micron, spread to almost several millimeters in wavelength. Therefore, infrared radiation refers to a wide band in the electromagnetic spectrum of radiant energy [1-6].

The electromagnetic spectrum is, in general, a function of both surface characteristics and temperature of the object. The surface effect on the electromagnetic spectrum is that the surface may be

---

\* To whom correspondence should be addressed

referred to as black, gray, diffuse or specular in radiation processes. Moreover, the electromagnetic spectrum is sensitive to the temperature in that the point of maximum on the curve will shift toward higher wavelengths at lower temperatures. Moreover, at lower temperatures, the maximum value of the curve also decreases. At higher temperatures, on the other hand, the summit of the curve, while increasing in value, will occur at lower wavelengths. This effect of temperature on the electromagnetic spectrum has two interesting results. The first is that the objects at high temperatures will exhibit visible light much more than those at low temperatures. In other words, high temperature objects can be seen by human eyes as a result of their own surface radiation of visible light. Low temperature bodies are, nevertheless, seen by our eyes just due to their surface reflection of incoming lights. The other result, however, refers to the infrared radiation. In fact, the infrared portion of the radiant energy exhibits much more significance in the electromagnetic spectrum of low temperature objects [8]. The significance of infrared radiation particularly at low temperatures suffices for its applicability in many industrial situations. The basis of many of these applications is thermography.

Thermography is a technique for temperature profiling of a surface. With thermography, the temperature distribution can be simply measured by taking photos from a surface using an infrared camera. The infrared camera senses the exiting thermal energy of a body and displays thermal images. The surface temperature profile is then determined as the intensity of the IR energy is directly related to the temperature of the surface [4]. This technique has many applications.

Failure in electrical distribution systems, deficiency in heat exchangers, and imperfection of insulations can be easily detected by thermography [7]. Loose contacts at electrical junctions or any other malfunction in an electrical system may lead to a considerable temperature rise in an area of the system. Deficiency in heat exchangers in a similar manner results in a considerable change in the surface temperature of heat exchanger elements. Thermal insulations, similarly, show considerable temperature change when destroyed. Tracing the temperature change and consequently the failure area in the system can be easily performed by the IR thermography.

Furthermore, level detection in storage tanks and even moisture detection in buildings are other applications of this technique [7]. Liquid level in storage tanks can be detected with the IR thermography by observing the temperature profile along the depth of the container. This occurs because of the thermal resistance difference between separate locations with and without the liquid. Moisture in buildings and roofs has a similar effect, and therefore, can be detected by the IR survey.

Moreover, objects in total darkness or dense atmosphere can be tracked using the infrared thermography. In darkness or when the atmosphere is very dense, the objects cannot be seen due to lack of visible light. An IR camera can be employed in these circumstances to provide thermal images of the objects being detected or traced.

There are several points which spell the advantages of the infrared thermography. While being fast and reliable, the IR thermography is a non-contact technique of temperature measurement. Moreover, a large surface area can be scanned by the IR camera in a very short time. Besides the various advantages, there are some however points that are considered as disadvantages of this technique. For example, its instrumental cost is high, and, the inside temperature of the body cannot be measured by the IR thermography [7].

Numerical methods, though not as reliable as experiments, are often convenient substitutes for them particularly when high cost or other shortcomings of the experimentation limit it from being fully carried out. Low cost, on the other hand, seems to be the most outstanding characteristic of numerical methods. With this superior characteristic, numerical approaches potentially have the capability of predicting the behavior of systems under the influence of different parameters input to them.

In this paper, a numerical simulation is conducted in order to predict infrared radiation exiting plain surfaces with different geometries. The numerical approach makes use of finite differences for the discretization of the equations governing the problem. The output of the numerical program is a series of images illustrating the infrared radiation distribution over the various surfaces under consideration. The results of this research will shed light on the prediction of the IR energy emitted from surfaces. In cases when an object is forbidden to be tracked by the IR camera, the results of the present research may be applicable.

## 2. Theory

This section includes the description of the numerical methodology adopted for the determination of infrared radiation distributed over plain surfaces.

The numerical methodology applied in the present work is basically of two parts. The first is to calculate the temperature distribution over the surface, and, the other is to evaluate the distribution of infrared radiation due the obtained temperature profile. So, the determination of the temperature profile is carried out before prediction of the IR energy exiting the surface.

Surfaces under consideration in the present numerical simulation are all assumed as plain with different geometries. A uniform amount of heat is assumed to be steadily generated in the surface. Heat generation in the surface is then conducted to the boundaries. The law of conservation of energy is therefore satisfied. The surface boundaries are all considered to be maintained at the temperature of the surroundings. The thermal conductivity of the surface is also assumed constant. With these assumptions, the governing equation of the problem is the two dimensional heat conduction equation. This equation along with its boundary condition is written below.

$$T_{xx} + T_{yy} + \frac{\dot{q}}{k} = 0, \quad (2.1)$$

$$T_{bound.} = T_{surr.}$$

In order to numerically solve the above equation for surfaces with different geometries, the surface should be divided into small elements, cells. Therefore, the physical domain of  $(x, y)$  coordinates is mapped into the computational domain of  $(\zeta, \pi)$  coordinates. In other words, the  $(x, y)$  curvilinear coordinate system is transformed into the Cartesian  $(\zeta, \pi)$  coordinates. Structured H grids are therefore provided for the surface. However, when the physical domain is mapped into the computational domain, the governing equation should also be transformed into the appropriate form of it in the new coordinate system. Therefore, with the coordinates assigned for the problem, Eqs (2.1) is transformed into the following equation [9].

$$\frac{1}{J^2} (\alpha T_{\zeta\zeta} - 2\beta T_{\zeta\pi} + \gamma T_{\pi\pi}) + (\nabla^2 \zeta) T_{\zeta} + (\nabla^2 \pi) T_{\pi} + \frac{\dot{q}}{k} = 0. \quad (2.2)$$

In Eq.(2.2),  $J$  is the Jacobean of the transformation. This parameter illustrates the variation of the old coordinate axes with respect to the new ones. The definitions of this parameter as well as  $\alpha$ ,  $\beta$  and  $\gamma$  are written below [9].

$$\alpha = x_{\pi}^2 + y_{\pi}^2,$$

$$\beta = x_{\zeta} x_{\pi} + y_{\zeta} y_{\pi},$$

$$\gamma = x_{\zeta}^2 + y_{\zeta}^2,$$

$$J = x_{\zeta} y_{\pi} - x_{\pi} y_{\zeta}.$$

(2.3)

The above differentials should be discretized in order to numerically solve the governing equation. Thus, central differences are used. In deriving the following relations, it should be kept in mind that the difference between two subsequent  $\zeta$  values is equal to unity. That is  $\zeta_{i+1} - \zeta_i = 1$ . Similarly, the difference between two successive  $\eta$  values is equal to unity. Therefore, for this coordinate it is true to write  $\eta_{j+1} - \eta_j = 1$ . With the foregoing point, the differentials of the physical domain coordinates with respect to the computational domain coordinates can be given as follows.

$$\begin{aligned}
 x_\zeta &= x_{i+\frac{1}{2},j} - x_{i-\frac{1}{2},j}, \\
 x_\eta &= x_{i,j+\frac{1}{2}} - x_{i,j-\frac{1}{2}}, \\
 y_\zeta &= y_{i,j+\frac{1}{2}} - y_{i,j-\frac{1}{2}}, \\
 y_\eta &= y_{i,j+\frac{1}{2}} - y_{i,j-\frac{1}{2}}.
 \end{aligned}
 \tag{2.4}$$

In the above equations, the fraction  $\frac{1}{2}$  is inserted because the central difference method is adopted for differentiation. However, with the above form of discretization, the parameters  $\alpha$ ,  $\beta$ , and  $\gamma$  along with the Jacobean,  $J$ , in Eq.(2.2) will be discretized as follows.

$$\begin{aligned}
 \alpha &= \left( x_{i,j+\frac{1}{2}} - x_{i,j-\frac{1}{2}} \right)^2 + \left( y_{i,j+\frac{1}{2}} - y_{i,j-\frac{1}{2}} \right)^2, \\
 \beta &= \left( x_{i+\frac{1}{2},j} - x_{i-\frac{1}{2},j} \right) \left( x_{i,j+\frac{1}{2}} - x_{i,j-\frac{1}{2}} \right) + \left( y_{i+\frac{1}{2},j} - y_{i-\frac{1}{2},j} \right) \left( y_{i,j+\frac{1}{2}} - y_{i,j-\frac{1}{2}} \right), \\
 \gamma &= \left( x_{i+\frac{1}{2},j} - x_{i-\frac{1}{2},j} \right)^2 + \left( y_{i+\frac{1}{2},j} - y_{i-\frac{1}{2},j} \right)^2, \\
 J &= \left( x_{i+\frac{1}{2},j} - x_{i-\frac{1}{2},j} \right) \left( y_{i,j+\frac{1}{2}} - y_{i,j-\frac{1}{2}} \right) - \left( x_{i,j+\frac{1}{2}} - x_{i,j-\frac{1}{2}} \right) \left( y_{i+\frac{1}{2},j} - y_{i-\frac{1}{2},j} \right).
 \end{aligned}
 \tag{2.5}$$

Equation (2.2), besides the above parameters, contains the partial differentials of  $T$  with respect to the new coordinates. Thus, differentials of  $T$  should be discretized as well. The discretization of the partial differentials of  $T$  given in Eq.(2.2) is then given in the following.

$$T_{\zeta\zeta} = T_{i+1,j} - 2T_{i,j} + T_{i-1,j},$$

$$T_{\zeta\eta} = \frac{1}{4} (T_{i+1,j+1} + T_{i-1,j-1} - T_{i+1,j-1} - T_{i-1,j+1}), \tag{2.6}$$

$$T_{\eta\eta} = T_{i,j+1} - 2T_{i,j} + T_{i,j-1}.$$

After the temperature profile is determined, the distribution of the infrared radiation exiting the surface is to be computed. For each cell of the surface, the emitted infrared radiation can be computed using the following equation [8].

$$IR = F\delta A\varepsilon\sigma T^4. \tag{2.7}$$

In this equation, IR, in Watts, is the infrared radiation exiting the elemental area,  $\delta A$ , of the cell. Moreover,  $\sigma$  is the Stefan-Boltzmann constant equal to  $5.67 \times 10^{-8} W / m^2 K^4$  and  $\varepsilon$  is the emissivity of the surface. The surface is assumed to be diffuse, gray. Therefore, the emissivity is considered constant in this work. Furthermore,  $T$  is the absolute temperature, already calculated, of the cell.  $F$  in this equation is, however, the fraction of the radiation of the cell which is in the range of infrared. Thus,  $F$  is determined from the equation given below [8].

$$F = \frac{1}{\sigma T^4} \left( \int_0^{\lambda_2} e_{\lambda b}(\lambda) d\lambda - \int_0^{\lambda_1} e_{\lambda b}(\lambda) d\lambda \right) \tag{2.8}$$

where  $\lambda_1$  and  $\lambda_2$ , respectively, denote the wavelengths of the beginning and the end of infrared band in the radiation spectrum. In Eq.(2.8),  $e_{\lambda b}$  is the spectral emissive power of black body calculated by Plank's distribution equation [8].

$$e_{\lambda b}(\lambda, T) = \frac{2\pi c_1}{\lambda^5 \left( e^{c_2/\lambda T} - 1 \right)}. \tag{2.9}$$

In Eq.(2.9),  $c_1$  and  $c_2$  are constants which have the following definitions [8].

$$c_1 = hc_0^2, \tag{2.10}$$

$$c_2 = \frac{hc_0}{K}.$$

Moreover,  $h$  in Eq.(2.10) is Plank's constant that is equal to  $6.62 \times 10^{-34}$ . Furthermore,  $K$  is equal to  $1.38 \times 10^{-23}$ . Also,  $c_0$  is the speed of light in vacuum. That is  $c_0 = 3 \times 10^8 m/s$  [8].

The integral in Eq.(2.8) should also be evaluated numerically. The following relation is given to evaluate this integral for the approximation of  $F$ .

$$F = \frac{15}{\pi^4} \sum_{n=1}^{\infty} \left( \frac{e^{-nz}}{n} \left( z^3 + \frac{3z^2}{n} + \frac{6z}{n^2} + \frac{6}{n^3} \right) \right). \tag{2.11}$$

In the above summation,  $z$  is equal to  $\frac{c_2}{\lambda T}$ . This summation should be carried out to approximate the fraction,  $F$ , of the energy emitted from the surface which is in the form of infrared radiation. However, the index  $n$  in this summation, may vary until a finite number such as 10 or even less.

The results of the present work will be presented in the next section.

### 3. Results

This section includes the results of the present numerical simulation. Surfaces with different geometries are considered and their emitted IR energy is presented in figures. In all the cases, the uniform heat generation is equal to  $100W/m^3$  and the thermal conductivity of the surface is assumed equal to  $100W/mK$ . The first surface considered is a square of edges equal to unity. The grid generated for this surface is shown in Fig.1.

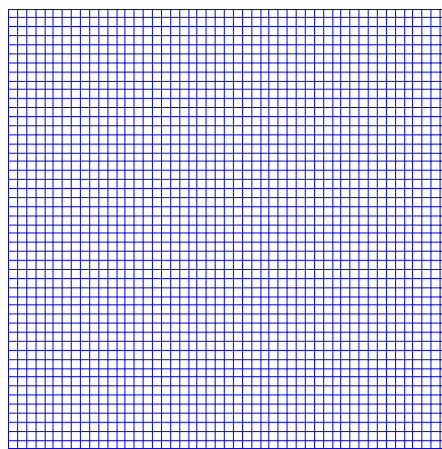


Fig.1. Grid generation provided for the square.

With the assumptions already stated, the temperature distribution of the surface is illustrated in Fig.2. As expected, it is seen from this figure that the maximum value of temperature occurs at the center of the square. Moreover, it can be inferred from the figure that the difference between the maximum and the minimum values of temperature is approximately  $60K$ .

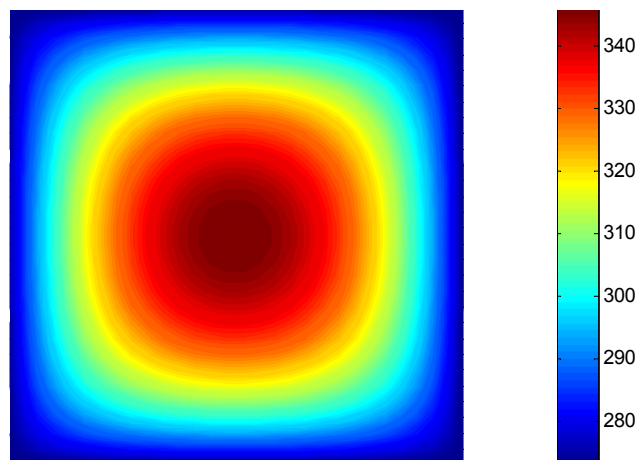


Fig.2. Temperature distribution of the surface.

Infrared radiation of the surface is shown in Fig.3. In calculating the IR distribution of the surface, the emissivity is assumed equal to 0.3. Values of  $\lambda_1$  and  $\lambda_2$  are also assumed equal to  $0.7 \mu m$  and  $1 mm$ , respectively. It can be seen from the figure that, similar to the temperature distribution, the maximum value of IR of the surface takes place at its center.

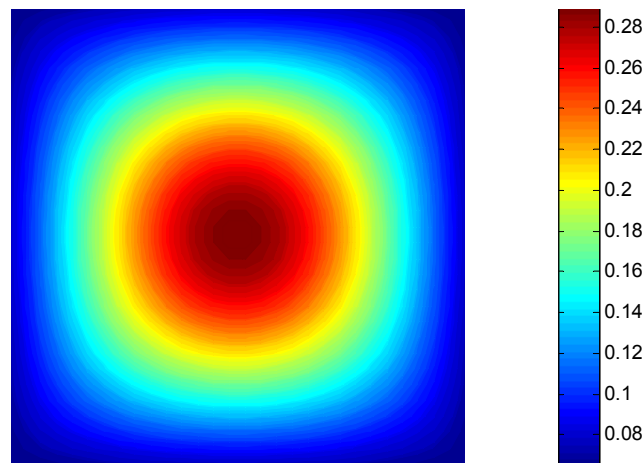


Fig.3. IR energy emitted from the surface.

The temperature distribution of a rectangular surface with the area equal to unity and aspect ratio of 4 is shown in Fig.4. An interesting result, by comparison of this figure with Fig.2, is that the maximum value of temperature in the rectangle is less than that for the square having the same value of area. The reason is that while the areas of both surfaces are equal, the perimeter of the rectangle is more than that of the square. Since the rate of the heat transfer has a direct relationship with the heat transfer area, this result can be proved.

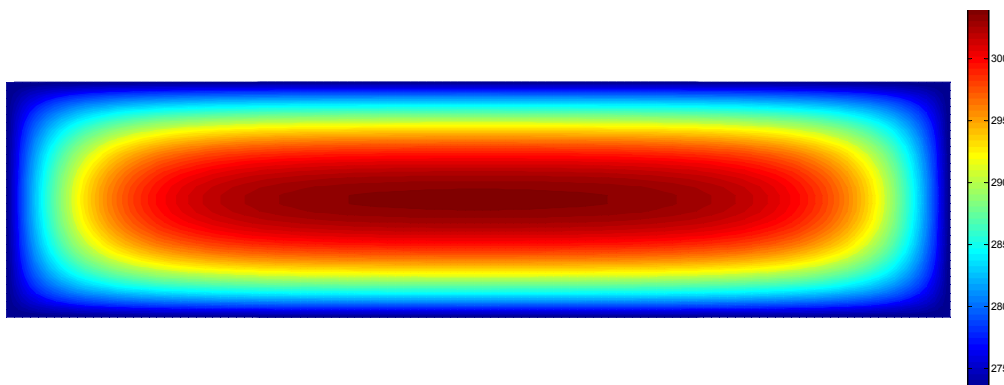


Fig.4. Temperature distribution of the rectangular surface.

After the temperature distribution of the surface is determined, the distribution of the infrared radiation is imaged in Fig.5. Similar to the result given for the maximum value of temperature, the maximum value of infrared radiation of the surface also reduces in comparison with its counterpart for the square.

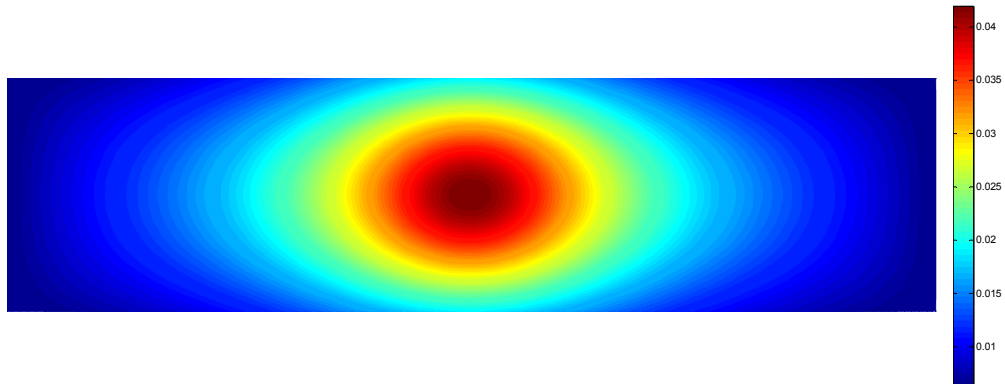


Fig.5. IR energy emitted from the surface.

Fig.6 illustrates the grid generation provided for a circular surface with the radius equal to  $0.56$ . This value is adopted for the radius of the circle in order to, similar to the previous surfaces, equalize its area to unity.

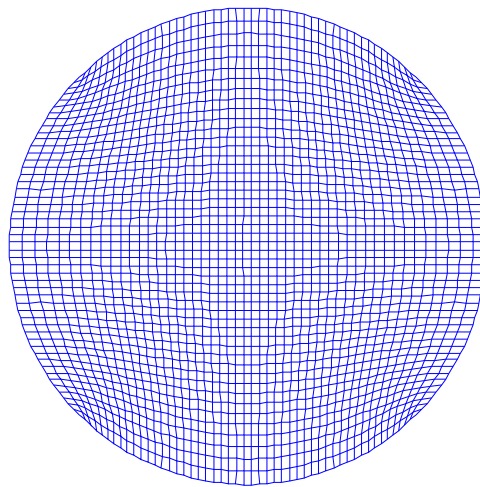


Fig.6. Grid generation provided for the circular surface.

The same amount of heat is assumed to be steadily and uniformly generated in this surface. The temperature distribution of this surface is shown in Fig.7. It can be seen from this figure that the maximum value of temperature in a circular surface is a little more than that of the square. The reason is that the perimeter of the circle is a little less than the perimeter of the square.

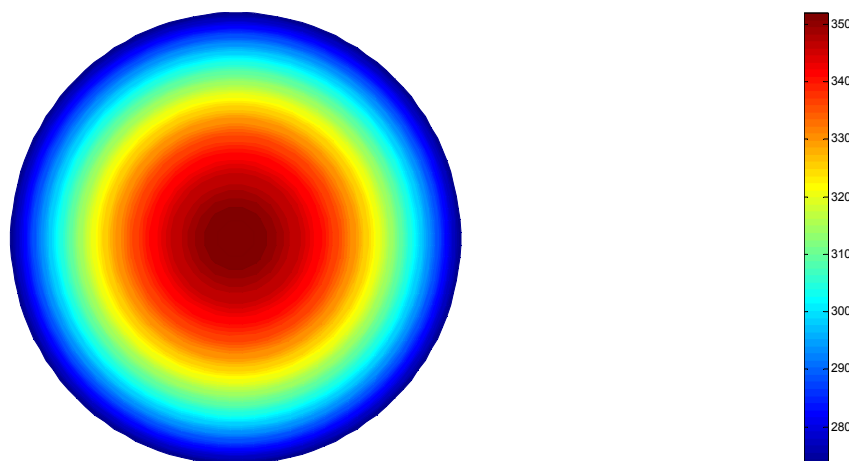


Fig.7. Temperature distribution of the surface.

Moreover, the distribution of the emitted infrared energy from the circular surface is shown in Fig.8. Similar to the case of the maximum temperature value, the value of maximum IR in this surface is slightly more than its counterpart in the square.

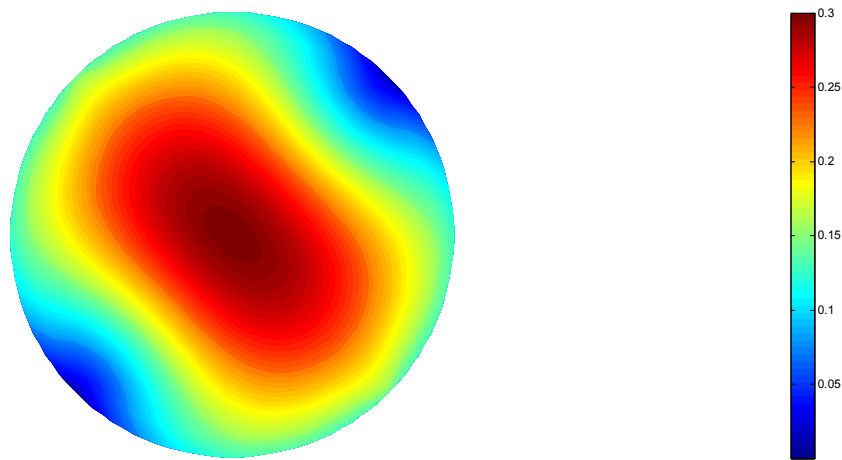


Fig.8. IR energy emitted from the surface.

Fig.9 illustrates the grid generation of type H provided for a trapezoidal surface. This shape given to the surface may simply simulate the side view of a ship.

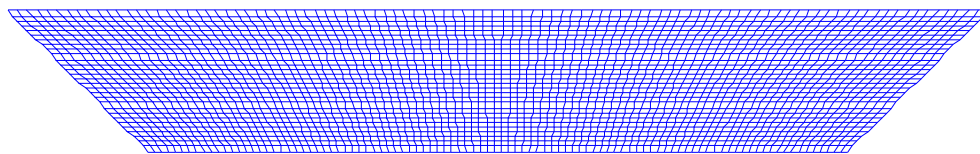


Fig.9. Grid generation provided for the trapezoidal surface.

The temperature distribution of the trapezoidal surface is given in Fig.10. Moreover, the distribution of infrared radiation emitted from the surface is shown in Fig.11.

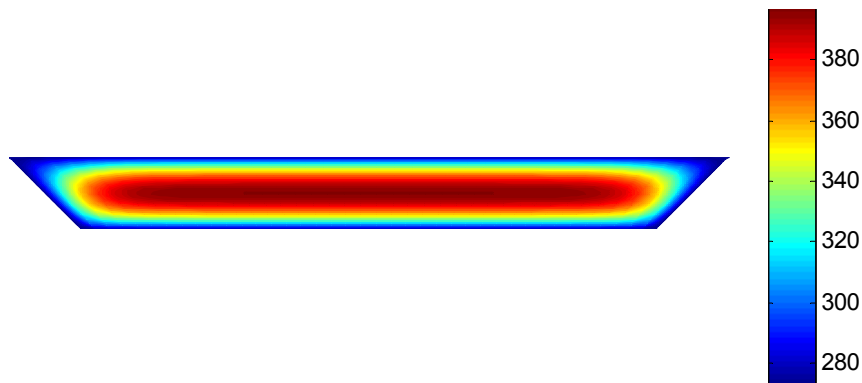


Fig.10. Temperature distribution of the surface.

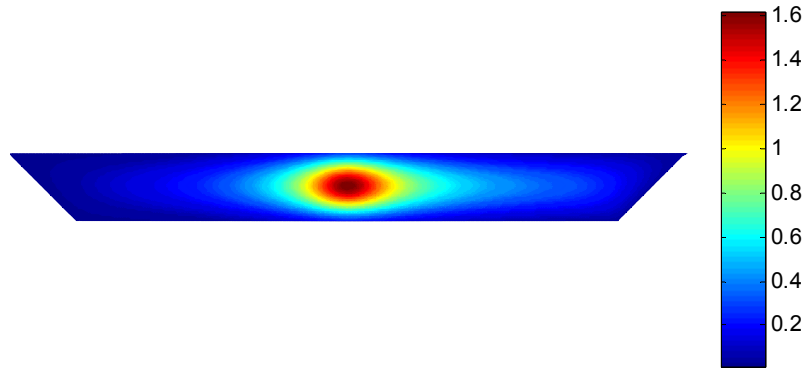


Fig.11. IR energy emitted from the surface.

Fig.12 shows a geometry which can simulate the deck of a ship. Although there are several formulas in the literature that simulate the deck of ships, in this figure arcs BH and AH are assumed as arcs of a circle. The geometrical values are given in the figure.

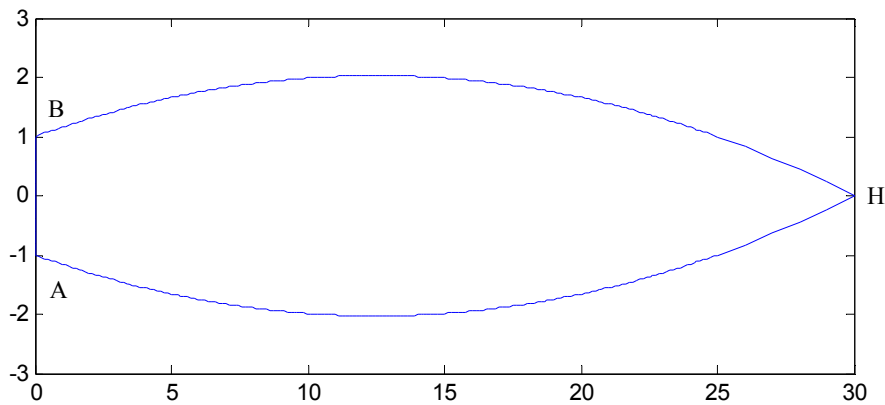


Fig.12. Geometry of a deck.

The temperature distribution of the above geometrical surface assuming the uniform heat generation is illustrated in Fig.13.

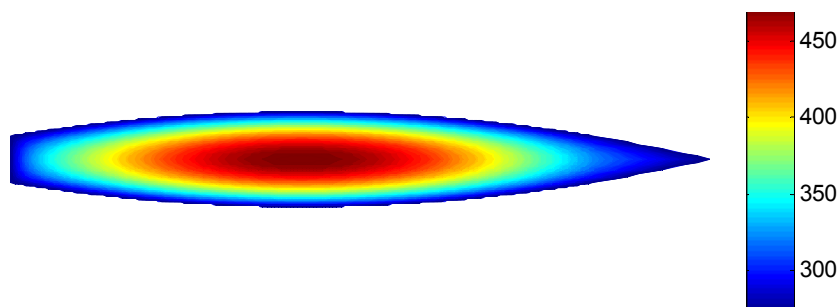


Fig.13. Temperature distribution of the surface.

The distribution of infrared radiation of the surface is also shown in Fig.14.

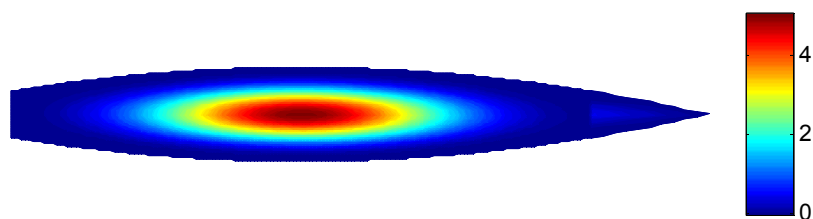


Fig.14. IR energy emitted from the surface.

#### 4. Conclusions

In this paper, a numerical simulation was performed in order to predict the infrared radiation distribution from plain surfaces with different geometries. Uniform heat was assumed to be steadily generated in the surfaces while their boundaries were considered to be at the temperature of the surroundings. The governing equation was solved using finite differences and the results were presented in the form of thermal and IR images. However, the following points are listed as the conclusions of the present work.

First, the maximum value of temperature, under present circumstances, occurs to be at the center of the surface.

Second, since the maximum value of temperature is found at the center of the surface, the maximum value of infrared radiation exiting the surface also happens at its center.

Third, for surfaces with equal values of area, the one having the largest perimeter has the minimum value of temperature at its center.

Forth, among surfaces all of the same area, the one with the largest value of area has the smallest value of infrared radiation in the center.

Fifth, in order to prevent a surface to be detected by IR camera, it can be covered by some material with low emissivity. Low emissivity materials are poor in radiation especially for emitting thermal energy and therefore are well suited for this purpose.

#### Nomenclature

- $c_0$  – speed of light in vacuum
- $e_{\lambda b}$  – spectral emissive power of black body
- $h$  – Plank's constant
- IR – Infrared Radiation
- $J$  – Jacobean of the transformation
- $x, y$  – curvilinear coordinate system
- $\zeta, \eta$  – Cartesian coordinates system
- $\lambda$  – wave length
- $\sigma$  – Stefan-Boltzmann constant
- $\nabla^2$  – Laplace operator

#### References

- [1] Skouro liakou A.S., Seferis I., Sianoudis I., Valais I., Fragopoulou A.F. and Margaritis L.H. (2014): *Infrared Thermography Imaging: Evaluating surface emissivity and skin thermal response to IR heating*. – E-Journal of Science and Technology, vol.3, pp.9-14.

- [2] Mahulikar S.P., Rao G.A., Sonawane H.R. and Prasad H.S.S. (2009): *Infrared Signature Studies of Aircraft and Helicopters*. – PIERS Proceedings, Moscow, Russia, August 18-21.
- [3] Clark M.R., McCann D.M. and Forde M.C. (2003): *Application of infrared thermography to the non-destructive testing of concrete and masonry bridges*. – NDT&E International 36, pp.265–275.
- [4] Nasr A. (2012): *Infrared Radiation*. – Ed. V. Morozhenko (InTech 2012) pp.95–126.
- [5] Hildebrandt C., Raschner C. and Ammer K. (2010): *An overview of recent application of medical infrared thermography in sports medicine in Austria*. – Sensors, vol.10, pp.4700-4715.
- [6] Kad R.S. (2013): *IR thermography is a Condition Monitor Technique in industry*. – International Journal of Advanced Research in Electrical, Electronics and Instrumentation Engineering, vol.2, No.3.
- [7] Garnaik S.P. (2000): *Thermography-A Condition Monitoring Tool for Process Industries*. – Seminar on Condition Monitoring & Safety Engineering for Process Industries, February 14-15.
- [8] Seigel R. and Howell J.R. (1992): *Thermal Radiation Heat Transfer*. – Third edition. Taylor and Francis Inc.
- [9] H<sup>a</sup>user J. (1996): *Modern Introduction to Grid Generation*. – EPF Lausanne, 23-27 September.

Received: October 31, 2016

Revised: June 17, 2017.